



ACADEMIC  
PRESS

Available online at [www.sciencedirect.com](http://www.sciencedirect.com)

SCIENCE @ DIRECT®

Journal of Solid State Chemistry 172 (2003) 123–126

JOURNAL OF  
SOLID STATE  
CHEMISTRY

<http://elsevier.com/locate/jssc>

# Compressibility of CaZrO<sub>3</sub> perovskite: Comparison with Ca-oxide perovskites

N.L. Ross<sup>a,\*</sup> and T.D. Chaplin<sup>b</sup>

<sup>a</sup> Department of Geological Sciences, Crystallography Laboratory, Virginia Polytechnic Institute and State University, Blacksburg, VA 24061, USA

<sup>b</sup> Department of Chemistry, University College London, Gower Street, London WC1E 6BT, UK

Received 30 July 2002; received in revised form 29 October 2002; accepted 9 November 2002

## Abstract

The evolution of the unit-cell parameters of CaZrO<sub>3</sub> perovskite, an orthorhombic perovskite belonging to space group *Pbnm*, have been determined to a pressure of 8.7 GPa at room temperature using single-crystal X-ray diffraction measurements. A fit of a third-order Birch–Murnaghan equation of state to the pressure–volume data yields values of  $V_0 = 258.04(2) \text{ \AA}^3$ ,  $K_{T0} = 154(1) \text{ GPa}$  and  $K'_0 = 5.9(3)$ . Although CaZrO<sub>3</sub> perovskite does not exhibit any phase transitions in this pressure range, the compression of the structure is anisotropic with [010] approximately 20% less compressible than either [100] or [001]. Compressional moduli for the unit cell parameters are:  $K_{a0} = 142(1) \text{ GPa}$  and  $K'_{a0} = 4.4(2)$ ,  $K_{b0} = 177(2) \text{ GPa}$  and  $K'_{b0} = 9.4(5)$ ,  $K_{c0} = 146(2) \text{ GPa}$  and  $K'_{c0} = 5.4(4)$ . Comparison with other orthorhombic Ca-oxide perovskites shows that there is systematic increase in compressional anisotropy with increasing distortion from cubic symmetry.

© 2003 Elsevier Science (USA). All rights reserved.

**Keywords:** CaZrO<sub>3</sub> perovskite; High pressure; Compressibility; Equation of state

## 1. Introduction

Many *ABO*<sub>3</sub> compounds with the perovskite structure exhibit orthorhombic *Pbnm* symmetry under ambient conditions and are isotypic with GdFeO<sub>3</sub>. Of this group of perovskites, the  $A^{2+}-B^{4+}$  perovskites are of particular interest to Earth scientists because the lower-mantle inventory of Mg<sup>2+</sup> and Ca<sup>2+</sup> is believed to be contained within the high-pressure silicate perovskites, MgSiO<sub>3</sub> and CaSiO<sub>3</sub>. Whereas MgSiO<sub>3</sub> perovskite is orthorhombic, CaSiO<sub>3</sub> perovskite is close to the ideal cubic structure [1], in which *B–O–B* angles between the corner-sharing [BO<sub>6</sub>] octahedra are 180° and the divalent  $A^{2+}$  cation resides in a dodecahedral site with *m3m* site symmetry, coordinated to 12 oxygens. However, CaSiO<sub>3</sub> perovskite becomes amorphous upon quenching to ambient conditions and can only be studied *in situ* at high pressures and temperatures. Other Ca-oxide perovskites, such as CaTiO<sub>3</sub>, CaGeO<sub>3</sub> and CaSnO<sub>3</sub>, are orthorhombic and display different degrees

of distortion from the ideal cubic structure. These distortions may be described in terms of the tilting of the [BO<sub>6</sub>] octahedra [2–3] which varies systematically with the size ratio of the cations occupying the dodecahedral and the octahedral site [4].

CaZrO<sub>3</sub> is an orthorhombic *Pbnm* perovskite consisting of slightly deformed ZrO<sub>6</sub> octahedra with Zr–O bond lengths ranging from 2.091(1) to 2.101(1) Å and O–Zr–O angles ranging from 88.0(1)° to 90.9(1)° [5]. The average Zr–O–Zr tilt angle between ZrO<sub>6</sub> octahedra is 146°, compared with 180° of the cubic perovskite structure. As shown in Fig. 1, the rotation of [ZrO<sub>6</sub>] octahedra distorts the Ca site with a reduction in site symmetry from *Pm3m* to  $\bar{1}$ , and the coordination of the Ca is reduced from 12 to 8 with Ca–O bond lengths ranging from 2.341 to 3.625 Å [5]. Among the orthorhombic Ca-oxide perovskites, CaZrO<sub>3</sub> perovskite is one of the most distorted and its high-pressure behavior is of special interest in light of the recent results for CaSnO<sub>3</sub> perovskite [6]. CaSnO<sub>3</sub> is an orthorhombic perovskite, belonging to space group *Pbnm*, with similar distortion from cubic symmetry as CaZrO<sub>3</sub> perovskite. The recent determination of the isothermal bulk modulus ( $K_{T0}$ ) of CaSnO<sub>3</sub> from single-crystal X-ray diffraction,

\*Corresponding author. Fax: +1-540-231-3386.

E-mail addresses: [nross@vt.edu](mailto:nross@vt.edu) (N.L. Ross), [ucfbtdc@ucl.ac.uk](mailto:ucfbtdc@ucl.ac.uk) (T.D. Chaplin).

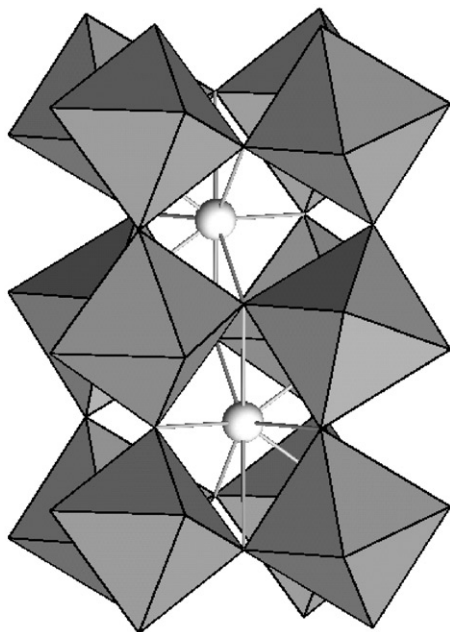


Fig. 1. Structure of  $\text{CaZrO}_3$  perovskite viewed down  $[110]$ . Ca atoms (spheres) reside in the cavities formed by the  $[\text{ZrO}_6]$  octahedral framework.

163(1) GPa, is significantly greater than previously measured and predicted from the bulk modulus-density trend of other Ca-oxide perovskites [6]. In a continuing study of the high-pressure behavior of Ca perovskites, we report here the equation of state and axial moduli of  $\text{CaZrO}_3$  perovskite using high-pressure, single-crystal X-ray diffraction and compare the results with other Ca-oxide perovskites.

## 2. Experimental methods

A powder sample of  $\text{CaZrO}_3$  perovskite was synthesized by mixing stoichiometric amounts of CaO and  $\text{ZrO}_2$  and heating at 1673 K over a period of 5 days interspersed with mechanical mixing until complete reaction was achieved. Single crystals were synthesized by pressurizing the powder sample in a sealed Pt capsule at 4 GPa and 1573 K for 5 h in a multi-anvil press. A single crystal suitable for high-pressure study was chosen on the basis of optical quality and diffraction quality. The high-pressure measurements were performed with a BGI-design diamond-anvil cell [7] using T301 steel as a gasket. The  $100 \times 80 \times 40 \mu\text{m}$  crystal was loaded into the diamond-anvil cell together with a ruby chip for approximate pressure measurements and a quartz crystal as an internal diffraction pressure standard. A 4:1 mixture of methanol:ethanol was used as the pressure-transmitting medium. The constant widths of the diffraction peaks at all pressures indicated that this pressure medium remained hydrostatic up to the highest pressure achieved, 8.7 GPa. Diffraction

Table 1  
Unit cell parameters of  $\text{CaZrO}_3$  perovskite between room pressure and 8.7 GPa

$P$ (GPa)	$a$ (Å)	$b$ (Å)	$c$ (Å)	Vol (Å <sup>3</sup> )
0.0001	5.5889(2)	5.7607(2)	8.0151(8)	258.02(3)
0.823(5)	5.5783(1)	5.7529(1)	7.9999(4)	256.69(1)
1.719(4)	5.5672(1)	5.74295(9)	7.9846(4)	255.29(1)
2.451(3)	5.5581(1)	5.7355(1)	7.9714(5)	254.12(2)
3.116(3)	5.5500(1)	5.7292(1)	7.9605(3)	253.12(1)
3.568(3)	5.5444(1)	5.7251(1)	7.9532(3)	252.45(1)
4.271(5)	5.5368(1)	5.7189(1)	7.9424(4)	251.49(2)
5.061(4)	5.5276(1)	5.7121(1)	7.9300(4)	250.38(1)
5.656(5)	5.52089(7)	5.70721(6)	7.9218(2)	249.607(8)
5.992(4)	5.5173(1)	5.70437(9)	7.9164(3)	249.15(1)
6.873(5)	5.5076(1)	5.6968(1)	7.9029(3)	247.96(1)
7.654(4)	5.49919(7)	5.69079(6)	7.8921(2)	246.983(8)
8.192(5)	5.4935(2)	5.6868(1)	7.8849(6)	246.33(2)
8.725(5)	5.48844(8)	5.68293(8)	7.8774(3)	245.70(1)

Numbers given in parenthesis represent 1 esd of last figure shown.

measurements were performed on a Huber four-circle diffractometer. Full details of the instrument and the peak-centering algorithms are provided by Angel et al. [8,9]. Unit-cell parameters were determined at each pressure from a least-squares fit to the corrected setting angles of 18–20 reflections obtained by the eight-position centering method [10]. The values of symmetry-constrained unit-cell parameters obtained by vector-least-squares [11] are reported in Table 1. Pressures were determined from the unit-cell volumes of the quartz crystal in the diamond anvil cell [8]. Equation of state parameters were obtained by a weighted-least-squares fit of the Birch–Murnaghan third-order equation (Eq. (1)) to the pressure–volume data. Weights for each datum were calculated by the effective variance method [12] from the esd in the unit-cell volume combined with the uncertainty in pressure corresponding to the esd of the unit-cell volume of the quartz pressure standard.

## 3. Results and discussion

Both the volume and the unit cell parameters of  $\text{CaZrO}_3$  perovskite decrease smoothly with increasing pressure, with no evidence of any phase transitions to 8.7 GPa (Figs. 2 and 3). Indeed, on the basis of the axial compression (Fig. 3), there is no indication that a phase transition will occur at higher pressures. A fit of the pressure–volume data (Table 1) to a third-order Birch–Murnaghan equation of state

$$P = \frac{3K_{T0}}{2} \left[ \left( \frac{V_0}{V} \right)^{7/3} - \left( \frac{V_0}{V} \right)^{5/3} \right] \times \left\{ 1 + \frac{3}{4}(K'_0 - 4) \left[ \left( \frac{V_0}{V} \right)^{2/3} - 1 \right] \right\} \quad (1)$$

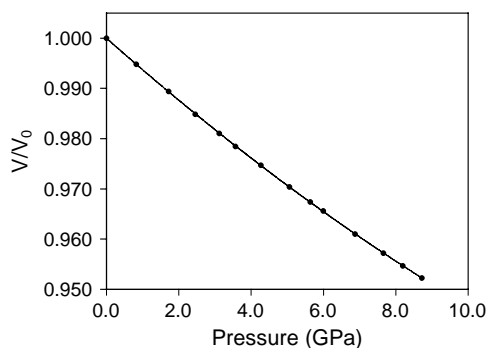


Fig. 2. Variation of the unit cell volume of  $\text{CaZrO}_3$  perovskite between room pressure and 8.7 GPa. The size of symbol shown represents  $\pm 1$  esd of measured  $V/V_0$ .

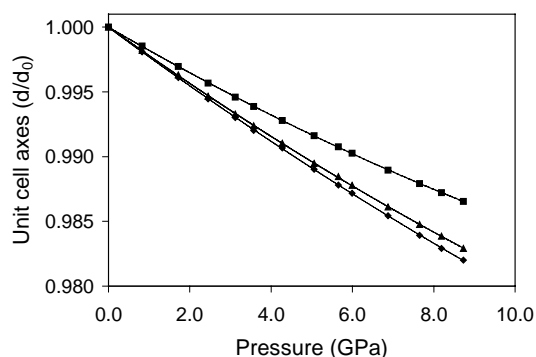


Fig. 3. Variation of unit cell parameters of  $\text{CaZrO}_3$  perovskite between room pressure and 8.7 GPa. The axes are represented by the following symbols:  $a/a_0$  (diamonds),  $b/b_0$  (squares) and  $c/c_0$  (triangles).

Table 2

Elastic moduli of orthorhombic Ca-oxide perovskites determined from high-pressure, single-crystal X-ray diffraction

Perovskite	$K_{T0}$ (GPa)	$dK_T/dP$	$K_a$ (GPa)	$K_b$ (GPa)	$K_c$ (GPa)	Ref.
$\text{CaGeO}_3$	194(2)	6.1(5)	195(5)	188(4)	204(3)	[13]
$\text{CaTiO}_3$	171(1)	6.6(3)	169(2)	168(2)	175(2)	[13]
$\text{CaSnO}_3$	163(1)	5.6(3)	148(1)	189(2)	156(2)	[6]
$\text{CaZrO}_3$	154(1)	5.9(3)	142(1)	177(2)	146(2)	This study

yields  $V_0 = 258.04(2) \text{ \AA}^3$ ,  $K_{T0} = 154(1) \text{ GPa}$ , and  $K'_0 = 5.9(3)$  where  $K'_0 = dK_T/dP$ . These data are compared with other orthorhombic,  $Pbnm$   $\text{CaBO}_3$  perovskites, where  $B = \text{Sn, Ti, and Ge}$ , in Table 2. The volumes and unit-cell parameters of all of these  $Pbnm$  perovskites show a smooth decrease with increasing pressure at room temperature with no phase transitions observed over the pressure ranges studied [6,13]. All of these perovskites have  $dK_T/dP$  close to 6. As shown in Fig. 4, the isothermal bulk moduli ( $K_{T0}$ ) of the Ca-oxide perovskites fall on a single smooth trend with inverse molar volume,  $V_m$ . At larger unit-cell volumes (i.e., at lower atom packing densities) the bulk modulus is

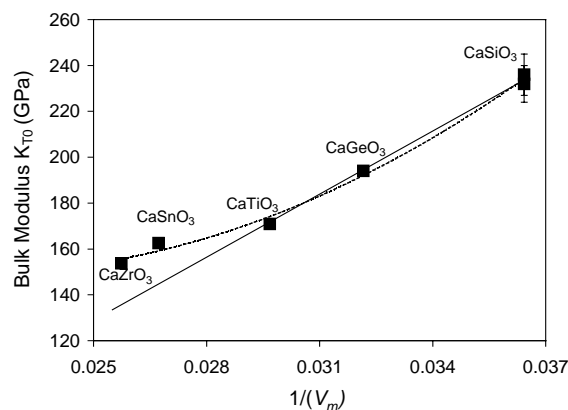


Fig. 4. Isothermal bulk moduli of Ca-oxide perovskites plotted as a function of inverse specific volume,  $1/V_m$ . The bulk moduli of  $\text{CaSiO}_3$  are from powder X-ray diffraction experiments [20,21]. The linear trend shown was previously reported from results of ultrasonic measurements [6,22] and single-crystal X-ray diffraction experiments [6,13].

smaller and the perovskites are softer. In general, the relationship between bulk moduli and specific volume is linear, i.e.,  $KV_m = \text{constant}$ , for simple oxide structures in which no phase transitions occur [14]. Indeed, a linear trend of  $K_{T0} = 9277/V_m - 104.4 \text{ GPa}$  was proposed for Ca-oxide perovskites on the basis of ultrasonic and X-ray diffraction measurements [13]. As shown in Fig. 4, however, the trend of  $K_{T0}$  with  $1/V_m$  of the Ca-oxide perovskites displays significant curvature with both  $\text{CaZrO}_3$  and  $\text{CaSnO}_3$  lying above the previously reported linear trend. The structural reason for the anomalous stiffening of  $\text{CaZrO}_3$  (and  $\text{CaSnO}_3$ ) relative to the other Ca perovskites might be related to the degree of structural distortion within these phases. One measure of the distortion from the ideal cubic structure is reflected in the tilt angles between the octahedra,  $\langle B-O1-B \rangle$  and  $\langle B-O2-B \rangle$ , which are both  $180^\circ$  in the cubic prototype.  $\text{CaGeO}_3$  is the least distorted of these perovskites with an average  $\langle B-O-B \rangle$  tilt angle of  $160^\circ$  [4], followed by  $\text{CaTiO}_3$  which has an average tilt angle of  $156^\circ$  [15],  $\text{CaSnO}_3$  with  $147^\circ$  [16] and  $\text{CaZrO}_3$  which has an average tilt angle of  $146^\circ$  [5]. If the dominant compression mechanism within these structures is volume reduction via tilting of rigid octahedra, then the anomalous stiffness of  $\text{CaZrO}_3$  and  $\text{CaSnO}_3$  might be the result of the tilts approaching some limiting value, as is observed in some tetrahedral framework structures [17].

The elastic moduli of the individual unit-cell axes of  $\text{CaZrO}_3$  perovskite were obtained from the measured data by fitting a third-order Birch–Murnaghan equation of state to the cubes of each of the cell parameters [18]. The resulting axial moduli ( $K_{a0}$ ) and their pressure derivatives ( $K'_{a0}$ ) are:  $K_{a0} = 142(1) \text{ GPa}$ ,  $K_{b0} = 177(2) \text{ GPa}$ , and  $K_{c0} = 146(2) \text{ GPa}$  with  $K'_{a0} = 4.4(2)$ ,  $K'_{b0} = 9.4(5)$ , and  $K'_{c0} = 5.4(4)$ . The maximum aniso-

ropy in the compressional moduli is thus about 20% with [010] being less compressible than both [100] and [001], which display similar compressibilities. It is noteworthy that in the progression from the least distorted orthorhombic perovskite,  $\text{CaGeO}_3$ , to the most distorted,  $\text{CaZrO}_3$ ,  $K_a$  and  $K_c$  decrease steadily whereas  $K_b$  changes the least (Table 2). Both the  $a$  and  $c$  parameters soften by  $\sim 30\%$ , compared to the overall 20% reduction in  $K_{T0}$ . As a consequence of the compressibility of the  $b$  parameter changing the least, [010] becomes significantly stiffer than either [100] or [001] in  $\text{CaZrO}_3$  compared to  $\text{CaGeO}_3$  perovskite. The net result is an increase in anisotropy in the compressional moduli to  $\sim 21\%$  in  $\text{CaZrO}_3$  and  $\text{CaSnO}_3$  compared to  $\text{CaGeO}_3$  and  $\text{CaTiO}_3$  which show a maximum of  $\sim 8\%$  anisotropy.

The axial compression behavior of  $\text{CaZrO}_3$  perovskite is similar to that observed in  $\text{MgSiO}_3$  perovskite, in which [010] is  $\sim 23\%$  less compressible than either [100] or [001] [19]. Similar to  $\text{CaZrO}_3$  perovskite, the latter display similar compressibilities, with  $a$  being slightly more compressible than  $c$ . In  $\text{MgSiO}_3$  perovskite, compression of the structure is achieved through *both* bond length reduction and increased rotation of the  $\text{SiO}_6$  octahedra [19]. More than one compression mechanism may also be operative in  $\text{CaZrO}_3$  perovskite at high pressure. The differences observed in the axial moduli of the Ca-oxide perovskites may therefore reflect different structural responses to pressure from the less-distorted structures to the more distorted structures.

#### 4. Conclusions

We have measured the equation of state of  $\text{CaZrO}_3$  perovskite and found it displays anomalous stiffening (higher bulk modulus) than previously predicted, but consistent with recent results for  $\text{CaSnO}_3$  perovskite. Systematic trends are observed among the axial compressibilities of orthorhombic Ca-oxide perovskites with [100] and [001] becoming more compressible as the degree of distortion from cubic symmetry increases. The [010] direction changes the least and the net result is a 3-fold increase in anisotropy in the compressional moduli. Work is in progress to determine whether the differences in compression observed among Ca-oxide perovskites reflect different structural responses to pressure, through

either bond compression and/or tilting of the octahedra comprising the corner-linked framework.

#### Acknowledgments

NLR gratefully acknowledges support from NSF grant EAR-0105864. TDC acknowledges support from the NERC grant GR3/11764.

#### References

- [1] H.K. Mao, L.C. Chen, R.J. Hemley, A.P. Jephcoat, Y. Wu, *J. Geophys. Res. Sect. B* 94 (1989) 17889–17894.
- [2] A.M. Glazer, *Acta Crystallogr. Sect. B* 28 (1972) 3384–3392.
- [3] P.M. Woodward, *Acta Crystallogr. Sect. B* 53 (1997) 32–43.
- [4] S. Sasaki, C.T. Prewitt, R.C. Liebermann, *Am. Mineral.* 68 (1983) 1189–1198.
- [5] H.J.A. Koopmans, G.M.H. van de Velde, P.J. Gellings, *Acta Crystallogr. Sect. C* 39 (1983) 1323–1325.
- [6] J. Kung, R.J. Angel, N.L. Ross, *Phys. Chem. Miner.* 28 (2000) 35–43.
- [7] D.R. Allan, R. Miletich, R.J. Angel, *Rev. Sci. Instrum.* 67 (1996) 840–842.
- [8] R.J. Angel, D.T. Allan, R. Miletich, L.W. Finger, *J. Appl. Crystallogr.* 30 (1997) 461–466.
- [9] R.J. Angel, R.T. Downs, L.W. Finger, in: R.M. Hazen, R.T. Downs (Eds.), *High-Temperature and High-Pressure Crystal Chemistry Reviews in Mineralogy and Geochemistry*, Vol. 41, Mineralogy Society of America, Washington DC, 2000, pp. 559–596.
- [10] H.E. King, L.W. Finger, *J. Appl. Crystallogr.* 12 (1979) 374–378.
- [11] R.L. Ralph, L.W. Finger, *J. Appl. Crystallogr.* 15 (1982) 537–539.
- [12] J. Orear, *Am. J. Phys.* 50 (1982) 912–916.
- [13] N.L. Ross, R.J. Angel, *Am. Mineral.* 84 (1999) 277–281.
- [14] D.L. Anderson, O.L. Anderson, *J. Geophys. Res.* 75 (1970) 3494–3500.
- [15] S. Sasaki, C.T. Prewitt, J.D. Bass, W.A. Sculze, *Acta Crystallogr. Sect. C* 43 (1987) 1668–1674.
- [16] A. Vegas, *Acta Crystallogr. Sect. B* 42 (1986) 167–172.
- [17] W.H. Baur, *J. Solid State Chem.* 97 (1992) 243–247.
- [18] R.J. Angel, in: R.M. Hazen, R.T. Downs (Eds.), *High-Temperature and High-Pressure Crystal Chemistry, Reviews in Mineralogy and Geochemistry*, Vol. 41, Mineralogy Society of America, Washington, DC, 2000, pp. 35–60.
- [19] N.L. Ross, R.M. Hazen, *Phys. Chem. Miner.* 17 (1990) 228–237.
- [20] Y. Wang, D.J. Weidner, F. Guyot, *J. Geophys. Res. Sect. B* 101 (1996) 661–672.
- [21] S.H. Shim, T.S. Duffy, G.Y. Shen, *Phys. Earth Planet. Inter.* 120 (2000) 327–338.
- [22] R.C. Liebermann, L.E.A. Jones, A.E. Ringwood, *Phys. Earth Planet. Inter.* 14 (1977) 165–178.